High-Resolution Weighted Range Point Migration Method for Fast 3-Dimensional Imaging with Ultra Wideband Radar

Takuya Sakamoto, Toru Sato,
Graduate School of Informatics, Kyoto University
Yoshida-Honmachi, Sakyo-ku, 606-8501 Kyoto, Japan

Pascal Aubry and Alexander Yarovoy
Delft University of Technology
Mekelweg 4, 2628CD Delft, the Netherlands

***Abstract*— Revised range point migration is a fast, noise-tolerant technology for ultra wide-band imaging. One important application of this technology is security systems to detect concealed weapons in security-controlled places such as train stations or airports. Such systems require higher resolution to distinguish weapons from benign objects or artifacts. In this paper, we propose a modified weighting function for the range point migration method that suppresses sharp amplitude changes due to the interference of multiple scattering waveforms. We apply the proposed method to numerical data to investigate its resolution and performance. We then apply the method to measurement data, which were obtained from a mannequin to demonstrate its imaging capability in a realistic scenario. By introducing this weighting function, results show remarkable improvement in resolution and image quality.**

I. Introduction

Because of its high range resolution and penetration, ultra-wide-band (UWB) radar imaging is a promising technology for next-generation security systems. A variety of imaging methods for UWB radar systems have been proposed [1], [2], [3], [4], [5], [6], [7]. One essential requirement for real-time security systems is computational speed, but many of the conventional imaging methods are unable to satisfy this requirement.

To attain adequate computational speed, we developed the reversible inverse boundary scattering transform (IBST) [10], [11], [12], [13] that gives the location of a scattering center using the antenna location and delay time of echoes without intensive computation. The IBST needs the derivative of the delay time function in terms of the antenna position. This differential operation is, however, unstable and too sensitive to noise and interference. To overcome this issue, the revised range point migration (RPM) method [8], [9] was developed, which applies a weighted average using all the neighboring peak points to calculate the derivative values stably.

The revised RPM method has been demonstrated to be fast and stable through computer simulations and measurements [9]. However, security systems designed to detect weapons require even higher resolution to reduce the false alarm rate and miss rate. The image resolution of the revised RPM is compromised by the interference of multiple echoes. In this paper, we propose a modified weighting function to suppress this interference effect. We demonstrate the improved imaging capability of the proposed method with computer simulations and measurements.

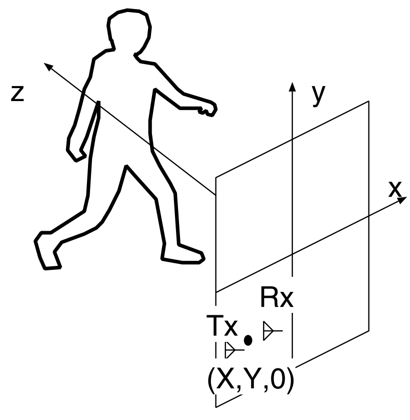

Fig. 1. System model with a pair of antennas scanning in the $(z = 0)$ plane.

II. System Model

We deal with a three-dimensional UWB radar imaging system. Figure 1 shows the system model assumed in this study. The measurement system consists of a transmitter-receiver pair positioned in the $z = 0$ plane along the x axis at a fixed distance $2d$. The midpoint between the transmitter and receiver is labeled $(X, Y, 0)$. With the transmitter-receiver pair being rastered at discrete intervals across a portion of the $z = 0$ plane, UWB pulses are transmitted and pulse echoes are received. The received signals contain not only echoes from the target but also a coupling signal propagating directly from the transmitter to the receiver. To eliminate this coupling signal, the background signal, measured without the target prior to the actual measurement, is subtracted from the received signal. Given antennae midpoint $(X, Y, 0)$, the signal received is labeled $s(X, Y, Z)$, where $Z = ct/2$. Here, c is the speed of the electromagnetic wave and t is the time interval between transmission and reception.

III. 3-D Bistatic IBST

This section describes the procedures of the 3-D bistatic IBST [14], the basis of the revised RPM method. First, we

2013 IEEE Radar Conference (RadarCon13)
978-1-4673-5794-4/13/$31.00 ©2013 IEEE

extract signal peaks, which satisfy

$$\frac{\partial}{\partial Z} s(X,Y,Z) = 0, \tag{1}$$

$$|s(X,Y,Z)| > T_{\rm s}, \tag{2}$$

where $T_{\rm s}$ is a constant threshold introduced to prevent noise being picked up. These peaks are indexed as (X_i, Y_i, Z_i) for $(i = 1, 2, \cdots, N)$. The corresponding amplitudes of these peaks are for simplicity denoted $s_i = s(X_i, Y_i, Z_i)$. For a single simple-shaped target, these points are easily connected sequentially to form multiple curved surfaces $Z(X, Y)$. This function is called a quasi-wavefront.

Next, we apply the following bistatic-IBST to the quasi-wavefronts to obtain images.

$$x = X - \frac{2Z^3 Z_X}{Z^2 - d^2 + \sqrt{(Z^2-d^2)^2 + 4d^2 Z^2 Z_X^2}}, \tag{3}$$

$$y = Y + Z_Y \left\{ d^2 (x-X)^2 - Z^4 \right\} / Z^3, \tag{4}$$

$$z = \sqrt{Z^2 - d^2 - (y-Y)^2 - \frac{(Z^2-d^2)(x-X)^2}{Z^2}}, \tag{5}$$

using for simplicity $Z_X = \partial Z/\partial X$ and $Z_Y = \partial Z/\partial Y$.

The bistatic-IBST requires accurate values of X, Y, Z, Z_X and Z_Y, of which X, Y and Z are known. To obtain derivatives Z_X and Z_Y, signal peaks need to be correctly connected. Since this is not an easy task for complex-shaped targets, we defer using the bistatic-IBST.

IV. Revised RPM Method

The RPM method [8] was developed to mitigate difficulties with the SEABED algorithm. To further enhance the processing speed, the revised RPM method [9] was proposed to sidestep the time-consuming optimization process used in the conventional RPM method. This method employs a weighting average to quickly and accurately estimate the derivative of the delay time. The relative orientation of peaks around the i-th peak is estimated with a weighted average as

$$\theta_i = \frac{\sum_{j \neq i, Y_j = Y_i} w_{i,j} \tan^{-1}\left(\frac{Z_i - Z_j}{X_i - X_j}\right)}{\sum_{j \neq i, Y_j = Y_i} w_{i,j}}, \tag{6}$$

where the weighting function $w_{i,j}$ is defined as

$$w_{i,j} = |s_i s_j| \exp\left(-\frac{(X_i - X_j)^2}{\sigma_X^2} - \frac{(Z_i - Z_j)^2}{\sigma_Z^2}\right), \tag{7}$$

and $\left|\tan^{-1}\left(\frac{Z_i - Z_j}{X_i - X_j}\right)\right| < \pi/4$, and the summations are over pairs of peaks with the same sign in the second derivative i.e.

$$s_{zz}(X_i, Y_i, Z_i) s_{zz}(X_j, Y_j, Z_j) > 0, \tag{8}$$

where $s_{zz}(X,Y,Z) = \frac{\partial^2}{\partial Z^2} s(X,Y,Z)$.

From this, we can estimate the partial derivative of the i-th range point in terms of X as $Z_X = \tan(\theta_i)$. In a similar way, we can estimate Z_Y. Finally, these derivatives are substituted into Eqs. (3), (4), and (5), to obtain target images.

V. Proposed Weighted Revised RPM Method

In this section, we propose a modified weighting function for the revised RPM method. In received signals for multiple targets, the interference of two or more waveforms makes it difficult to extract peak points. However, we can use the fact that the amplitude along the wavefront changes sharply only around the intersection of multiple echoes. We propose an interference suppression method based on this characteristic.

In the proposed method, the revised weighting function $w'_{i,j}$ is defined as follows. If $|s_i/s_j| < 1$ then

$$w'_{i,j} = |s_i/s_j|^p \, |s_i s_j| \exp\left(-\frac{(X_i - X_j)^2}{\sigma_X^2} - \frac{(Z_i - Z_j)^2}{\sigma_Z^2}\right). \tag{9}$$

Otherwise,

$$w'_{i,j} = |s_j/s_i|^p \, |s_i s_j| \exp\left(-\frac{(X_i - X_j)^2}{\sigma_X^2} - \frac{(Z_i - Z_j)^2}{\sigma_Z^2}\right). \tag{10}$$

In short, the amplitude ratio of s_i and s_j is incorporated in the weighting function, where a sharp amplitude change suppresses the weight. In this way, signals with a sharp amplitude change due to interference do not contribute to the final image, mitigating the resolution deterioration due to interference. We use this weighting function w' instead of w in the following sections. We have empirically chosen $p = 25$, although the results are not sensitive to this parameter. The conventional method corresponds with $p = 0$.

VI. Performance Evaluation

We evaluate the calculation time and image quality of the original weighting function and the proposed weighting function in simulations. The following parameters are assumed in this section. The distance between the antennas is 5.5 cm, giving $d = 2.75$ cm. The antennas scan from locations at 1.0 cm intervals ranging $-37.0\text{cm} \leq X \leq 37.0\text{cm}$ and $-75.0\text{cm} \leq Y \leq 75.0\text{cm}$. The total number of measuring points are $75 \times 151 = 11,325$. The revised RPM method extracts 20 peaks for each antenna position. We set $\sigma_X = \sigma_Y = 0.8\text{cm}$ and $\sigma_Z = 0.3\text{cm}$. The i-th target image point (x_i, y_i, z_i) obtained from Eqs. (3), (4) and (5) is weighted with amplitude $|s_i|$ to generate an image. Although the revised RPM method generates three-dimensional images, we show two-dimensional projection images. The volume image $I_{\rm v}(x,y,z)$ is projected onto the x-y plane by

$$I(x,y) = \int |I_{\rm v}(x,y,z)| {\rm d}z. \tag{11}$$

The grid sizes for x, y and z in images are all 1.0 cm. The range of the depth z is calculated for $0 \leq z \leq 100.0$ cm.

First, we apply the revised RPM method and the proposed weighted revised RPM method to simulated data. Simulated data are generated assuming two point targets in the plane $z = 50$ cm, spaced at different intervals from 0 to 20 cm. The center frequency of the transmitted signal is 10.0 GHz and the 10-dB bandwidth is 10.4 GHz. Figures 2 and 3 are images generated with the conventional and proposed

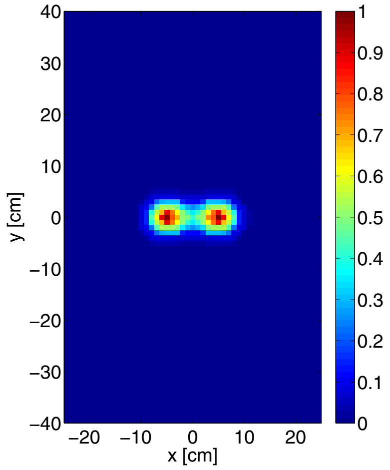

Fig. 2. Image generated with the conventional revised RPM method for two targets 10 cm apart.

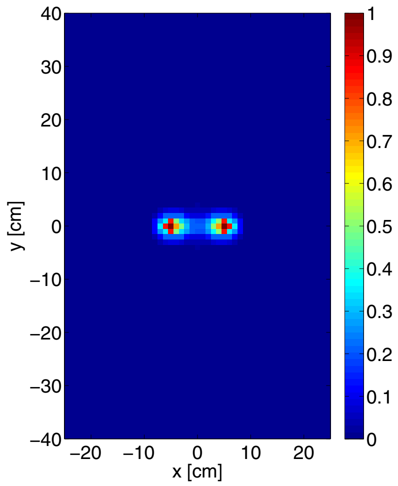

Fig. 3. Image generated with the proposed weighted revised RPM method for two targets 10 cm apart.

weighted revised RPM methods for a pair of targets located 10 cm apart. The figures show that the proposed method produces a clearer image than the conventional method.

Figures 4 and 5 display the sections of the images on the $y = 80$ cm plane for various target spacing from 0 to 20 cm for the conventional and proposed methods, respectively. The figures clearly show that the proposed method has higher resolution than the conventional method. The cross-range resolutions for the conventional and proposed methods are 10.0 cm and 8.0 cm, giving a 20% improvement in the cross-range resolution, where the resolution is defined by the half-power (-3 dB) points.

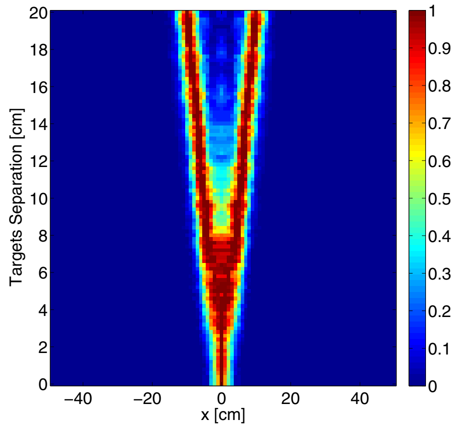

Fig. 4. Resolution analysis for the conventional revised RPM method.

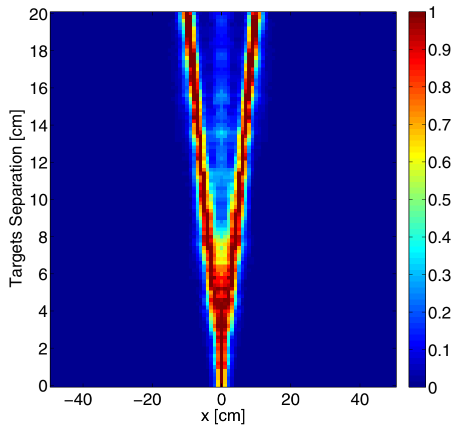

Fig. 5. Resolution analysis for the proposed weighted revised RPM method.

VII. Application to Measurement Data

We apply our proposed method to measurement data. A mannequin is placed 50 cm from the antennas. In the frequency band used in this study, the power reflection coefficient from a human body is high. Therefore, to model a human body, we substituted a metal-coated plastic mannequin. The antenna separation, scanning intervals and range are the same as in the previous section. Figure 6 is a photo of the mannequin used in our measurement. Figures 7 and 8 are the images generated by the conventional and proposed versions of the revised RPM.

As for the shoulders, the image quality of the proposed weighted RPM is not necessarily better than the conventional RPM. This is because the weight function used for the proposed method suppresses signals that suffer interference. Some information contained in the original data can be lost by this process, compromising the sensitivity. However, from other parts of the body including the torso and legs, the image generated with the proposed method is clearer than that with the conventional method. This demonstrates that under a

Fig. 6. Metal-coated mannequin for the measurement.

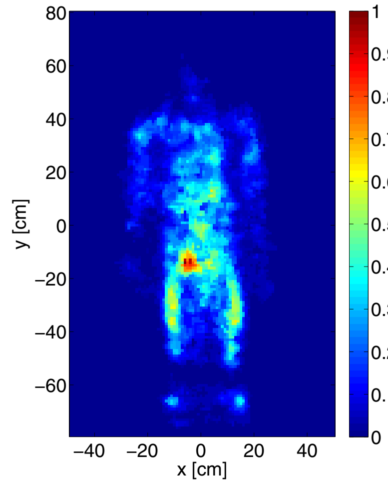

Fig. 7. Image generated with the conventional revised RPM method.

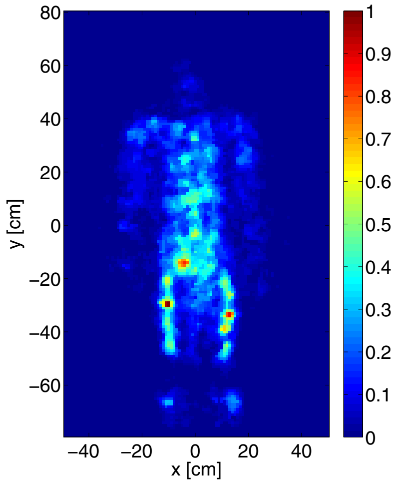

Fig. 8. Image generated with the proposed weighted revised RPM method.

certain condition, the proposed method is effective in obtaining clearer images from measurement data.

VIII. Conclusion

In this paper, we proposed a new imaging method, which is an extended version of the revised RPM method, for UWB radar systems to achieve resolution higher than that achieved with the conventional method. The resolution of the conventional revised RPM method is compromised by the superposition of multiple echoes. To overcome this problem, we introduced a modified weighting function that suppresses signal peaks with significantly different amplitude values. We evaluated the performance of the proposed imaging method by carrying out numerical simulations and measurements. In the simulation, we quantitatively investigated the resolution of the conventional and proposed methods. With the proposed method, the resolution improved from 10.0 cm to 8.0 cm, corresponding to a 20% of improvement. In the measurement, we used a metal-coated mannequin as a target to demonstrate the imaging capability for a complex-shaped target such as a human body. Both results suggest improvement of the resolution and imaging capability by introducing our new method.

References

[1] A. G. Yarovoy, T. G. Savelyev, P. J. Aubry, P. E. Lys, L. P. Ligthart, “UWB array-based sensor for near-field imaging,” IEEE Transactions on Microwave Theory and Techniques, vol. 55, no. 6, part 2, pp. 1288-1295, June 2007.

[2] X. Zhuge, A. G. Yarovoy, T. Savelyev, L. Ligthart, ”Modified Kirchhoff migration for UWB MIMO array-based radar imaging” IEEE Transactions on Geoscience and Remote Sensing, vol. 48, no. 6, pp. 2692–2703, 2010.

[3] X. Zhuge, and A. Yarovoy, ”A sparse aperture MIMO-SAR based UWB imaging system for concealed weapon detection,” IEEE Transactions on Geoscience and Remote Sensing, vol. 49 no. 1, pp. 509–518, 2011.

[4] Y. Wang, Y. Yang, A. E. Fathy, “Experimental assessment of the cross coupling and polarization effects on ultra-wide band see-through-wall imaging reconstruction,” IEEE MTT-S International Microwave Symposium Digest, pp. 9–12, June 2009.

[5] A. Nelander, “Switched array concepts for 3-D radar imaging,” Proc. 2010 IEEE Radar Conference, pp. 1019–1024, 2010.

[6] T. Counts, A. C. Gurbuz, W. R. Scott Jr., J. H. McClellan, and K. Kim, “Multistatic ground-penetrating radar experiments,” IEEE Trans. Geoscience and Remote Sensing, vol. 45, no. 8, pp. 2544–2553, Aug. 2007. 2008.

[7] Y. Yang and A. E. Fathy, “Development and implementation of a real-time see-through-wall radar system based on FPGA,” IEEE Trans. Geoscience and Remote Sensing, vol. 47, no. 5, pp. 1270–1280, May 2009.

[8] S. Kidera, T. Sakamoto and T. Sato, “Accurate UWB Radar 3-D Imaging Algorithm for Complex Boundary without Range Points Connections,” IEEE Trans. Geoscience and Remote Sensing, vol. 48, no. 4, pp. 1993–2004, 2010.

[9] T. Sakamoto, T. G. Savelyev, P. J. Aubry and A. G. Yarovoy, “Revised Range Point Migration Method for Rapid 3-D Imaging with UWB Radar,” Proc. 2012 IEEE International Symposium on Antennas and Propagation and USNC-URSI National Radio Science Meeting, 508.2, July 2012.

[10] T. Sakamoto, “A fast algorithm for 3-dimensional imaging with UWB pulse radar systems,” IEICE Trans. on Communications, vol. E90-B, no. 3, pp. 636–644, 2007.

[11] D. W. Winters, J. D. Shea, E. L. Madsen, G. R. Frank, B. D. Van Veen, S. C. Hagness, "Estimating the Breast Surface Using UWB Microwave Monostatic Backscatter Measurements," IEEE Transactions on Biomedical Engineering, vol. 55, no. 1, pp. 247–256, 2008.
[12] S. Hantscher, A. Reisenzahn, C. G. Diskus, "Through-Wall Imaging With a 3-D UWB SAR Algorithm," IEEE Signal Processing Letters, vol. 15, pp. 269–272, 2008.
[13] R. Salman, I. Willms, "In-Wall Object Recognition based on SAR-like Imaging by UWB-Radar," Proc. 8th European Conference on Synthetic Aperture Radar (EUSAR), 2010.
[14] S. Kidera, Y. Kani, T. Sakamoto and T. Sato, "A fast and high-resolution 3-D imaging algorithm with linear array antennas for UWB pulse radars," IEICE Trans. on Communications, vol. E91-B, no. 8, pp. 2683–2691, 2008.